

# Kinetic Investigations of Self-Condensing Group Transfer Polymerization

Peter F. W. Simon,<sup>\*1</sup> Axel H. E. Müller<sup>2</sup>

**Summary:** Hyperbranched methacrylates were synthesized by Self-Condensing Group Transfer Polymerization (SCGTP) of 2-(2-methyl-1-triethylsiloxy-1-propenyloxy)ethyl methacrylate (MTSHEMA) and characterized by multi-detector SEC as well as quantitative <sup>13</sup>C-NMR. Kinetic measurements revealed that side reactions limit the molecular weights and lower the polydispersity. A maximum degree of branching of  $DB \approx 0.4$  and a reactivity ratio,  $r = k_A/k_B = 18 \pm 5$ , was determined.

**Keywords:** GTP; hyperbranched; kinetics (polym.); NMR

## Introduction

For more than a decade hyperbranched polymers have been an attractive research area. They combine the features of a dendrimer-like dense structure and an exponentially increasing number of end groups with the ease of preparation of a linear polymer by means of a one-pot reaction.<sup>[1,2]</sup> Hyperbranched vinyl polymers can be yielded by self-condensing vinyl polymerization (SCVP) of initiator–monomers.<sup>[3]</sup> These are of a general AB<sup>\*</sup>-type structure, where A represents a polymerizable vinyl group and B<sup>\*</sup> stands for a group capable of initiating the polymerization of double bonds. Thus, the AB<sup>\*</sup>-molecule combines features of an initiator and a monomer and has therefore been named “inimer”.<sup>[4–7]</sup> This approach is analogous to the polycondensation of an AB<sub>2</sub>-monomer, which was first discussed by Flory.<sup>[8,9]</sup> In both cases the reaction between the same functional groups is not possible; in

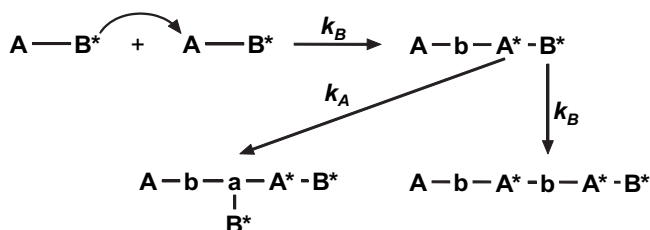
consequence the polyreactions result in hyperbranched polymers without the formation of any network.

The SCVP commences by attack of the activated initiating B<sup>\*</sup> group on the vinyl group of another inimer. This converts the second inimer's vinyl group, A, into a new type of propagating active group, A<sup>\*</sup>. The dimer possesses two active sites, A<sup>\*</sup> and B<sup>\*</sup>, one double bond, A, and one inactive group, b, stemming from the initiating moiety of the first inimer. Both, the initiating B<sup>\*</sup> moiety and the newly created propagating group, A<sup>\*</sup>, can react with any vinyl group, A, present in any inimer or polymer with rate constants  $k_A$  and  $k_B$ , respectively, cf. Scheme 1.<sup>[6,10,11]</sup>

Self-Condensing Vinyl Polymerization has been applied to a broad variety of living polymerization techniques, i.e. cationic,<sup>[3]</sup> ATRP<sup>[12–17]</sup>, nitroxide-mediated radical polymerization<sup>[18]</sup>, and even ring-opening polymerization.<sup>[19]</sup> Baskaran employed an anionic route to hyperbranched styrene derivatives by reacting an equimolar amount of 1,3-diisopropylbenzene and *n*-butyl lithium, thus forming an inimer *in situ*.<sup>[20]</sup> We<sup>[11,21]</sup> – and independently of us Sakamoto et al.<sup>[22]</sup> – used group transfer polymerization (GTP) of the inimer 2-(2-methyl-1-triethylsiloxy-1-propenyloxy)ethyl methacrylate (MTSHEMA) (**1**) where the silylketene acetal group can be activated by nucleophilic catalysts (cf. Figure 2)<sup>[23,24]</sup> to initiate GTP.<sup>[25,26]</sup>

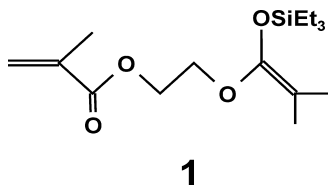
<sup>1</sup> GKSS Research Centre Geesthacht GmbH, Institute of Polymer Research, Max-Planck-Str. 1, D-21502 Geesthacht, Germany  
Fax: (+49) 4152 872466  
E-mail: peter.simon@gkss.de

<sup>2</sup> Makromolekulare Chemie II und Bayreuther Institut für Makromolekülforschung, Universität Bayreuth, D-95440 Bayreuth, Germany.  
Fax: (+49) 921 553393  
E-mail: axel.mueller@uni-bayreuth.de



### Scheme 1.

Basic Steps in Self-Condensing Vinyl Polymerization. Formation of a Dimer with Two Different Active Sites,  $A^*$  and  $B^*$  and of Two Distinct Trimers.



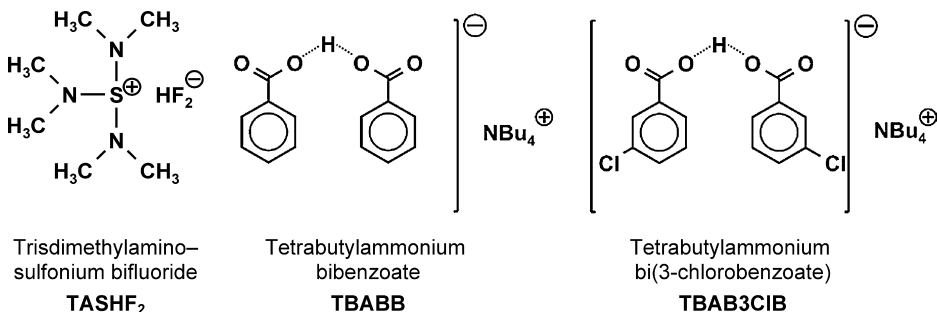
### Kinetic Results

The dependence of the molecular weight distribution on the conversion of MTSHEMA (**1**),  $x_1$ , for a batch polymerization was monitored by varying the absolute concentration of the inimer,  $I_0$ , as well as the type and concentration of the nucleophilic catalyst,  $C_0$ , (cf. Scheme 2 and Table 1) employed to activate the GTP reaction. The results are depicted in Figure 1.

For unequal reactivities of initiating  $B^*$  and propagating  $A^*$  groups,  $r = k_A/k_B \neq 1$ , the complete molecular weight distribution cannot be calculated analytically. Only the number averages are independent of the reactivity ratio,  $r$ .<sup>[6]</sup> Any other average

must be numerically determined. Because the reactivity ratio of the MTSHEMA system was found to be in the range  $10 < r < 40$  (*vide infra*), the theoretical dependence of the number-average degree of polymerization and the polydispersity as a function of the conversion of inimer,  $x_1$ , for  $r = 1$  and  $r = 100$  are shown for comparison in Figure 1 (a) and (b).

The scatter of the data in Figure 1 only allows to us draw qualitative hypotheses. For low conversions, the experimental values for  $M_n$  and  $M_w/M_n$  generally correspond to the theoretical predictions. For conversions  $x_1 \geq 0.9$ , however, the experimental data are always below the theoretical ones. It may be reasoned that this deviation is due to the unequal reactivity of the  $A^*$  and  $B^*$  centers as the reactivity ratio  $r = k_A/k_B$  influences the molecular weight distribution. As depicted in Figure 1 the case  $r > 1$  leads to an increase of the polydispersity index, making the discrepancy between theory and experiment even



### Scheme 2.

Nucleophilic GTP Catalysts.

**Table 1.**Kinetic Results of the SCGTP of MTSHEMA (**1**) in THF.

Symbol	Catalyst	$I_0/\text{mol L}^{-1}$	$C_0/\text{mol L}^{-1}$	$T/^\circ\text{C}$	$x_i$	$M_n$	$M_w/M_n$
□	TBAB <sub>3</sub> ClB	0.167	$1.67 \cdot 10^{-3}$	20	0.64	438	1.85
					0.92	691	2.43
					1	935	2.16
					1	775	2.44
					1	760	2.29
					1	676	2.28
◇	TBAB <sub>3</sub> ClB	0.167	$1.67 \cdot 10^{-3}$	0	0.38	743	2.47
					0.45	761	3.29
					0.80	827	2.38
					0.95	840	2.12
					1	864	1.92
△	TBAB <sub>3</sub> ClB	0.167	$1.67 \cdot 10^{-3}$	−20	0.06	364	1.13
					0.05	380	1.12
					0.19	343	1.52
					0.62	871	2.09
					0.86	1208	5.48
▽	TBAB <sub>3</sub> ClB	0.167	$1.67 \cdot 10^{-3}$	−40	0.01	213	1.11
					0.02	218	1.13
					0.03	245	1.31
					0.11	255	1.33
					0.21	260	1.52
▼	TBABB	0.146	$4.29 \cdot 10^{-5}$	0	0.81	2100	3.21
					0.79	4300	3.49
					0.87	3800	4.17
					0.99	3500	4.66
					1	4800	3.21
■	TBABB	0.142	$5.46 \cdot 10^{-5}$	−20	1	10600	3.56
					0.40	830	5.45
					0.78	1200	6.21
					0.89	2250	3.49
					0.94	2400	4.17
					0.97	2450	4.66

larger. Possible reactions which can explain this difference are (i) the backbiting reaction<sup>[27]</sup> and (ii) the cyclization reaction.<sup>[28,29]</sup>

### Side Reactions

The term “backbiting”<sup>[27]</sup> describes the nucleophilic attack of an active chain end to the penultimate carbonyl group yielding a cyclic β-ketoester. This species contains two new types of functional groups,  $a_{\text{CYC}}$  and C, respectively. Unlike in a linear architecture, backbiting detaches whole branches of the macromolecule in the case of a hyperbranched one thus lowering the final degree of polymerization<sup>[11,21]</sup>, cf. Scheme 3.

The resulting β-ketoester possesses an absorption maximum at  $\lambda \approx 300$  nm as detected from the cyclic trimer (**4**), cf. Scheme 4,<sup>[27]</sup> allowing an identification by

SEC-UV coupling methods. In SEC the UV( $\lambda = 300$  nm) signal corresponds to the number of β-keto-ester units present in the macromolecule, whereas the RI-signal is proportional to the polymer's weight. Accordingly, the amount of β-ketoester units can be judged from ratio of the molar mass-weighted UV( $\lambda = 300$  nm) and the RI signals,  $UV(\lambda = 300 \text{ nm}) \cdot M/RI$ . In Figure 2 two eluograms for reaction times of 1 min and 135 min are compared. For short reaction times, no significant UV absorption is detected, indicating the absence of backbiting. After 135 min the ratio  $UV(\lambda = 300 \text{ nm}) \cdot M/RI$  increases dramatically, especially for low elution volumes,  $V_e$ , demonstrating the occurrence of multiple backbiting reactions per macromolecule. Especially for high conversions, molecular weights increase slower with conversion of vinyl groups than predicted for a SCVP, cf.

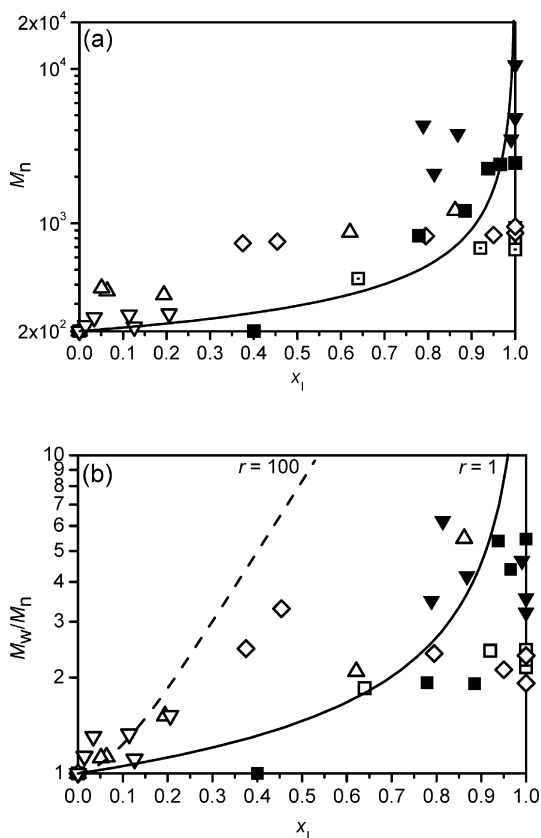
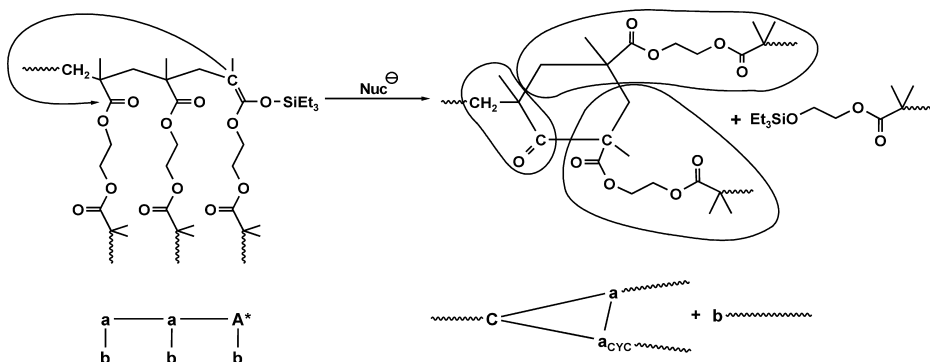


**Figure 1.**

Plot of (a) the number-average molecular weight,  $M_n$ , and (b) the polydispersity index,  $M_w/M_n$ , versus the conversion of inimer,  $x_i$ , for the SCGP of MTSHEMA (**1**). ( $\square$ ,  $\diamond$ ,  $\triangle$ ,  $\nabla$ ): TBAB<sub>3</sub>ClB,  $I_0 = 0.167 \text{ mol L}^{-1}$ ,  $C_0 = 1.67 \cdot 10^{-3} \text{ mol L}^{-1}$ ; ( $\blacksquare$ ):  $T = 20^\circ\text{C}$ , ( $\diamond$ ):  $T = 0^\circ\text{C}$ , ( $\triangle$ ):  $T = -20^\circ\text{C}$ , ( $\nabla$ ):  $T = -40^\circ\text{C}$ ; ( $\blacksquare$ ,  $\blacktriangledown$ ): TBABB; ( $\blacksquare$ ):  $I_0 = 0.142 \text{ mol L}^{-1}$ ,  $C_0 = 5.45 \cdot 10^{-5} \text{ mol L}^{-1}$ ,  $T = -20^\circ\text{C}$ ; ( $\blacktriangledown$ ):  $I_0 = 0.146 \text{ mol L}^{-1}$ ,  $C_0 = 4.29 \cdot 10^{-5} \text{ mol L}^{-1}$ ,  $T = 0^\circ\text{C}$ , cf. Table 1. For comparison the dependences for a ratio  $r=1$  (—) and  $r=100$  (---) were computed according to Figs. A3-1 and A4-1 of the supporting information of ref.<sup>[6]</sup> Note that unequal rate constants only affect the polydispersity index.



**Scheme 3.**

Example for the "Backbiting" Reaction in the GTP of MTSHEMA (**1**). Functional Groups and Chemical Structure of the Reaction Are Shown.

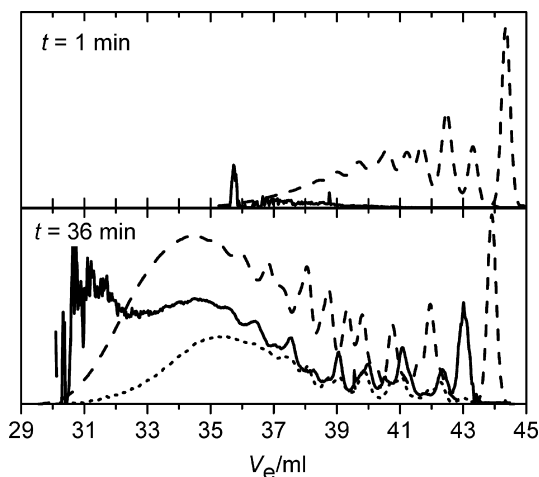


**Figure 2.**

SEC traces at reaction times (a) 1 min and (b) 135 min of a SCGTP of MTSHEMA. Reaction conditions:  $I_0 = 0.167$  mol/L,  $C_0 = 3.34 \cdot 10^{-4}$  mol/L, TBAB<sub>3</sub>ClB. (---): RI signal, (···): UV( $\lambda = 300$  nm), and (—): UV( $\lambda = 300$  nm).M/RI.

Figure 1. As vinyl groups are not affected in the formation of  $\beta$ -ketoesters, this finding cannot be explained by the occurrence of backbiting.

Vinyl groups may be consumed by an intramolecular reaction with an  $A^*$  or  $B^*$  group. This cyclization reaction yields multifunctional macro-initiators containing one loop. Because these do not contain a vinyl group, the reaction kinetics will be altered – an effect also studied theoretically for  $AB_2$  polycondensation using Monte-Carlo simulation.<sup>[28,29]</sup> This simulation predicts the fraction of cyclic  $x$ -mers to increase with increasing degree of polymerization,  $P_n$ , and overall conversion leading to a decrease in polydispersity<sup>[30–32]</sup> and finite number- and weight-average molecular weights even at complete conversion of vinyl-groups.<sup>[28,29]</sup> Consequently, the strong deviation in the kinetics of the SCGTP of MTSHEMA (**1**) from theoretical predictions, especially the occurrence of finite molecular weights in the limit  $x_1 = 1$ , are indirect indications for the occurrence of cyclization. The topology in the presence and the absence of cyclization only differs in the structure of one single group per macromolecule; hence a direct determination of cyclization can only be accomplished using advanced

mass-spectroscopy techniques as pointed out by Dušek et al.<sup>[28]</sup>

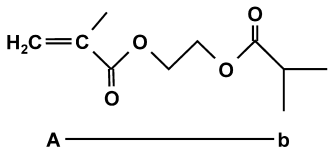
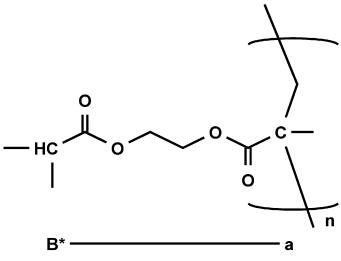
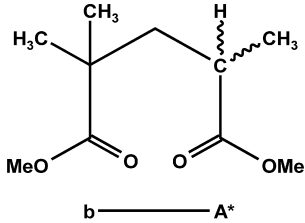
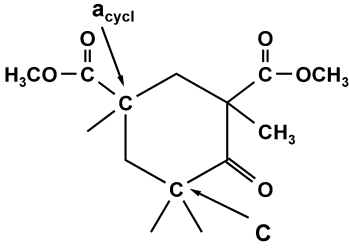
#### Determination of the Degree of Branching and the Reactivity Ratio

In order to estimate the shifts of the different groups present in hyperbranched PolyMTSHEMA (**poly-1**) model compounds were analyzed by  $^{13}\text{C}$ -NMR. The linear analogue poly(2-isobutylethyl methacrylate) (**poly-2**)<sup>[11,21,22–33]</sup> mimics the structural motif of the  $a$ - and  $B^*$ -moieties. The  $A^*$ -groups' chemical environment may be estimated from 2,2,4-trimethyl glutaric acid dimethyl ester (**3**).<sup>[34]</sup> The cyclic trimer of MMA 2,4-(dicarbomethoxy)-2,4,6,6-tetramethylcyclohexanone (**4**)<sup>[34]</sup> exhibits a pattern similar to the  $C$ - and  $a_{\text{cyc}}$ -moieties (cf. Scheme 3). The chemical shifts of the various functional groups composing the hyperbranched polymer are compiled in Scheme 4.

The degree of branching,  $DB$ , may be defined as

$$DB = \frac{2(\text{number of branched units})}{2(\text{number of branched units}) + (\text{number of linear units})} \quad (1)$$

The fraction of the structural units can be obtained from the product of the fractions of the active or reacted groups

<p>2-isobutyrylethyl methacrylate (2)</p>  <p><math>\delta/\text{ppm}</math>: 135 – 130</p>	<p>poly(2-isobutyrylethyl methacrylate) (poly-2)</p>  <p><math>\delta/\text{ppm}</math>: 34.0      46.0 to 45.0</p>
<p>2,2,4-trimethylglutaric acid dimethyl ester (3)</p>  <p><math>\delta/\text{ppm}</math>: 25.2      19.5 36.4</p>	<p>2,4-(dicarbomethoxy)-2,4,6,6-tetramethylcyclohexanone (4)</p>  <p><math>\delta/\text{ppm}</math>: 40.2      43.3</p>

**Scheme 4.**

Structure of the Model Compounds. Carbon Atoms Used for the Determination of the Chemical Shifts in  $^{13}\text{C}$ -NMR Are Designated with C in the Structure.

of which they consist of.<sup>[35]</sup> During the backbiting reaction  $a_{\text{CYC}}$  and C groups are generated, cf. Scheme 3. The C group has to be considered as a linear unit as the backbiting reaction does not create an additional branchpoint (cf. Scheme 3). Finally, the degree of branching,  $DB_{\text{NMR}}$ , using the intensities of  $^{13}\text{C}$ -INGATED NMR spectra reads

$$DB_{\text{NMR}} = \frac{2(a + a_{\text{CYC}})b}{2(a + a_{\text{CYC}})b + A^*b + (a + a_{\text{CYC}})B^* + C} \quad (2)$$

A typical inverse-gated decoupling (INGATED)  $^{13}\text{C}$ -NMR-Spectra at 100,6 MHz in  $\text{CDCl}_3$  of **poly-1** is depicted in

Figure 3. From that the fraction of the various functional groups was obtained by normalization of their intensity with respect to the  $(-\text{O}-\text{CH}_2-\text{CH}_2-\text{O}-)$  group. The results are given in Table 2

At full conversion further relations can be established<sup>[35]</sup>

$$a = B^* \quad \text{and} \quad b = 1 - B^*. \quad (3)$$

Defining a ratio of reacted groups

$$\Xi = \frac{a + a_{\text{CYC}}}{b}, \quad (4)$$

the fraction of initiating groups can be rewritten

$$B^* = \frac{\Xi}{\Xi + 1} \quad (5)$$

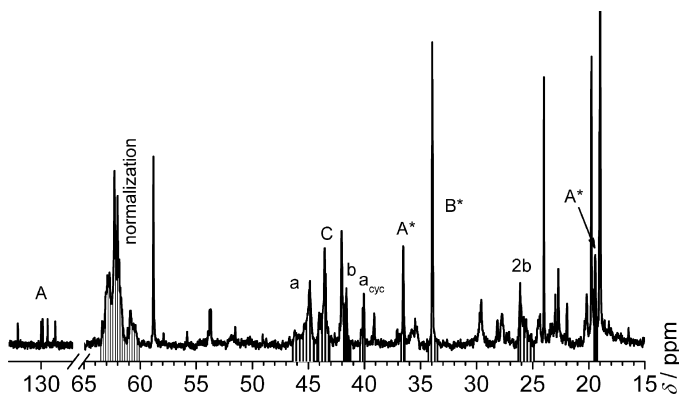


**Figure 3.**

Representative 100 MHz  $^{13}\text{C}$ -INGATED NMR-spectra of **poly-1**. Shaded areas were used to calculate the degree of branching,  $DB_{\text{NMR}}$ .

and used to calculate the theoretical reactivity ratio<sup>[35]</sup>

$$r_{\text{theo}} = \frac{B^*}{B^* - \ln B^* - 1} \quad (6)$$

Accordingly, the reactivity ratio at full conversion as determined from the NMR spectra,  $r_{\text{NMR}}$ , can be computed by combination of eqs. (5) and (6)

$$r_{\text{NMR}} = \frac{k_A}{k_B} = - \frac{\Xi}{1 + (1 + \Xi) \ln \left( \frac{\Xi}{1 + \Xi} \right)} \quad (7)$$

However, eq. (6) was originally derived for ideal SCVP conditions, i. e. absence of backbiting and cyclization. Only in that “ideal” case, the degree of branching,  $DB_{\text{theo}}$ , can be estimated from its depen-

dence on the reactivity ratio,  $r_{\text{theo}}$ .<sup>[13,15,35]</sup> In the case of **poly-1** the occurrence of backbiting and cyclization reactions makes this procedure erroneous.

The impact of the reaction conditions of the SCGTP of MTSHEMA (**1**) on the reactivity ratio,  $r_{\text{NMR}}$ , and the degree of branching,  $DB_{\text{NMR}}$ , are outlined in Table 2 including the results of Sakamoto's et al. study.<sup>[22]</sup> Because they did not publish any information on the fraction of structural units, we were not able to calculate the degree of branching using eq. (2). To establish a correlation to our results, we calculated a theoretical degree of branching,  $DB_{\text{theo}}$ , by neglecting the presence of backbiting (i. e. assuming  $r_{\text{NMR}} = r_{\text{theo}}$ ) and using the theoretical dependence given in Fig. 5 of ref.<sup>[6]</sup>

The results of Table 2 indicate a variance of the results of Sakamoto's group with ours. Probably, these differences are due to the precipitation of their polymers, which excludes lower molecular weight compounds from analysis. Moreover, Table 2 highlights the influence of the GTP-catalyst on the reactivity ratio,  $r$ , and the degree of branching,  $DB$ .

According to our results, the oxyanion-type catalyst leads to a higher reactivity ratio compared to the fluoride one. As the reaction rate of the oxyanions is generally lower due to a shift of the activation

**Table 2.**

Dependence of the Reactivity Ratio,  $r_{\text{NMR}} = k_A/k_B$ , and the Degree of Branching,  $DB_{\text{NMR}}$ , on the Reaction Conditions for the SCGTP of MTSHEMA (**1**).

Catalyst	$T/^\circ\text{C}$	$DB_{\text{NMR}}^{\text{b)}$	$r_{\text{NMR}}$	$DB_{\text{theo}}^{\text{c)}$
TBAB <sub>3</sub> ClB	−20	0.24	22.7	0.36
TBAB <sub>3</sub> ClB	0	0.38	19.4	0.38
TBAB <sup>b)</sup>	20		10.1	0.43
TASHF <sub>2</sub>	−20	0.42	13.4	0.41
TASHF <sub>2</sub>	0	0.25	13.1	0.42
TASHF <sub>2</sub> <sup>a)</sup>	20		38.1	0.31

a) results of Sakamoto et al.<sup>[22]</sup>

b) calculated using eq. (2).

c) obtained from the theoretical dependence  $DB = f(r)$  according to Fig. 5 of ref.<sup>[6]</sup>

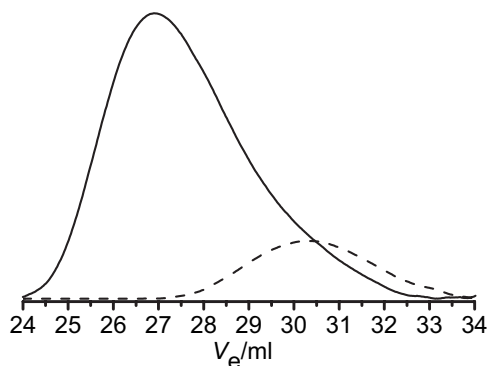


**Figure 4.**

GPC traces (RI-signal) of hyperstar polymer (—) and hyperbranched precursor (---). Molecular weight averages (universal calibration): hyperstar  $M_n = 10\,300$ ;  $D = 2.2$ ; precursor  $M_n = 2\,000$ ;  $D = 1.7$ .

equilibrium to the dormant species the deactivation process of the propagating groups,  $A^*$ , is not fast enough and vinyl addition can occur several times before the deactivation takes place. In the case of the more “silicophilic” fluoride catalyst, the deactivation process occurs faster, leading to more similar reactivities and consequently a higher degree of branching.

Direct exchange of activities between living and dormant chain ends may account for another explanation. This degenerative transfer is a well-known feature of the GTP influencing the molecular weight distribu-

tion as well as the reaction kinetics especially in the case of oxyanion catalysis.<sup>[36]</sup> It is therefore very likely that this transfer may also account for the “slower” deactivation process of the  $A^*$  groups.

#### Applications

Due to their high number of end groups hyperbranched polymers are potential candidates for multifunctional initiators.<sup>[11,12,18]</sup> The proof of concept in case of the addition of methyl methacrylate, MMA, to a living **poly-1** precursor is demonstrated in Figure 4. In the SEC trace

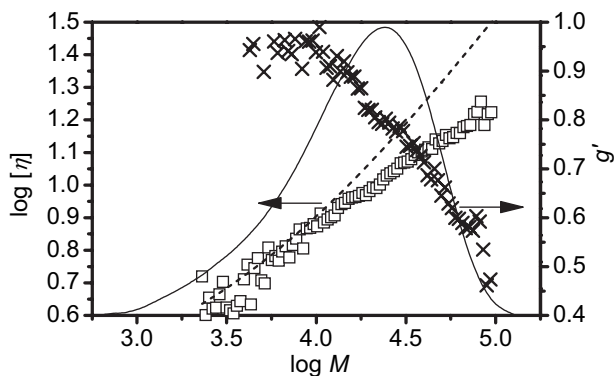


**Figure 5.**

Mark-Houwink Plot for hyperstar and linear PMMA. ( $\square$ ): Intrinsic viscosity of hyperstar; (---): linear PMMA ( $\alpha = 0.688$ ); (—): RI-signal; (X): contraction factors of hyperstar PMMA. The fit of the intrinsic viscosity of hyperstar PMMA yields a Mark-Houwink exponent of  $\alpha = 0.37$ .



the peak maximum of the resulting hyperstar molecule is shifted to lower elution volumes compared to the hyperbranched precursor, consequently its molecular weight averages (universal calibration, precursor  $M_n = 2\,000$ , i.e.  $P_n = 10$  and  $D = 1.7$ ; hyperstar  $M_n = 10\,300$  and  $D = 2.2$ ) are significantly increased. Since the number of active groups in SCVP equals  $P_n$ , an average of 10 arms with average arm length of  $M_{n,arm} = 830$  can be estimated for the hyperstar polymer.

From on-line viscosimetry Mark-Houwink plots and contraction factors  $g' = [\eta]_{br}/[\eta]_{lin}$  using linear PMMA for  $[\eta]_{lin}$  were established. The contraction factors decrease with increasing molecular weights demonstrating the densely packed structure. Furthermore, the branched architecture is corroborated by the low Mark-Houwink exponent of  $\alpha = 0.37$  (cf.  $\alpha = 0.688$  for linear PMMA<sup>[11]</sup>).

The copolymerization of MTSHEMA (**1**) with *tert*-butyl methacrylate, *t*BMA, yields highly branched PtBMA. According to Doherty and Müller<sup>[37]</sup> a controlled GTP of *t*BMA can only be achieved if the TASHF<sub>2</sub> catalyst is continuously added during the polymerization procedure.

The corresponding Mark-Houwink plot, Figure 6, clearly demonstrate the branched structure of the PtBMA synthesized. Acid-

catalyzed hydrolysis of the *tert*-butyl groups and neutralization with NaOH produces a water-soluble, highly branched poly(methacrylic acid) sodium salt.<sup>[10]</sup>

## Conclusion

The Self-Condensing Group Transfer Polymerization of the inimer MTSHEMA (**1**) leads to hyperbranched polymethacrylates. However, molecular weights are lower and the molecular weight distribution is narrower than predicted from the theory of Self-Condensing Vinyl Polymerization. As judged from kinetic data and SEC results, cyclization and backbiting are responsible for this effect. The degree of branching,  $DB$ , and reactivity ratios of the two active groups,  $r = k_A/k_B$ , were determined by quantitative <sup>13</sup>C-NMR spectroscopy. Reactivity ratios indicate a higher reactivity of the B\* group resulting in a  $DB < 0.5$ . The addition of MMA to a living hyperbranched precursor yields a densely packed structure as revealed by the corresponding Mark-Houwink plots. The copolymerization of the inimer MTSHEMA (**1**) with the comonomer *t*BMA, yields highly branched PtBMA which can be hydrolyzed to a highly branched polyelectrolyte.

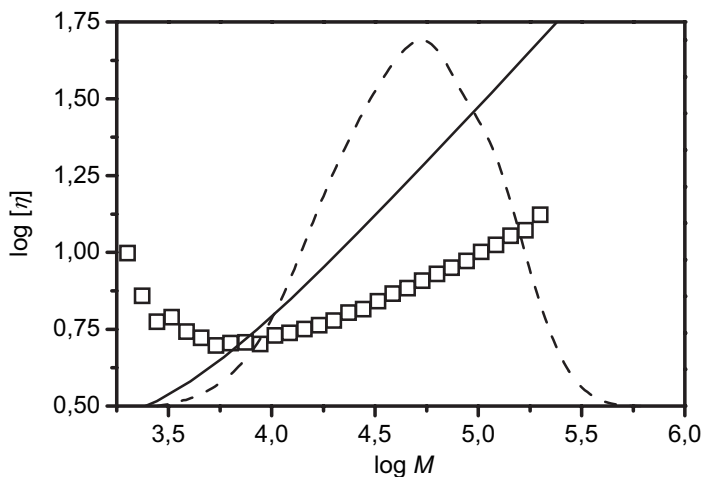


**Figure 6.**

Mark-Houwink plot (□) and RI signal (---) for highly branched poly(*tert*-butyl methacrylate). (—): intrinsic viscosity of linear PtBMA ( $\alpha = 0.752$ ).

**Acknowledgements:** This work was supported by the Deutsche Forschungsgemeinschaft. P.S. wishes to thank Peter Blumers, Mainz, for his helping hands in the laboratory. Finally, the authors are indebted to Dr. W. Radke, Darmstadt, for initializing their research activities on hyperbranched polymers.

- [1] H. Mori, A. H. E. Müller, *Prog. Polym. Sci.* **2003**, 28, 1403.
- [2] H. Mori, A. H. E. Müller, *Top. Curr. Chem.* **2003**, 228, 1.
- [3] J. M. J. Fréchet, M. Henmi, I. Gitsov, S. Aoshima, M. R. Leduc, R. B. Grubbs, *Science* **1995**, 269, 1080.
- [4] B. Hazer, *J. Macromol. Sci. Chem.* **1991**, A28(Suppl.1), 47.
- [5] B. Hazer, *Makromol. Chem.* **1992**, 193, 1081.
- [6] A. H. E. Müller, D. Yan, M. Wulkow, *Macromolecules* **1997**, 30, 7015.
- [7] J. E. Puskas, M. Grasmüller, *Macromol. Symp.* **1998**, 132, 117.
- [8] P. J. Flory, *J. Am. Chem. Soc.* **1953**, 74, 2718.
- [9] J. P. Flory, "Principles Of Polymer Chemistry", Cornell University Press, Ithaca, London, **1953**.
- [10] P. F. W. Simon, A. H. E. Müller, *Macromolecules* **2001**, 34, 6206.
- [11] P. F. W. Simon, A. H. E. Müller, *Macromolecules* **2004**, 37, 7548.
- [12] S. G. Gaynor, S. Edelman, K. Matyjaszewski, *Macromolecules* **1996**, 29, 1079.
- [13] M. W. Weimer, J. M. J. Fréchet, I. Gitsov, *J. Polym. Sci., Part A: Polym. Chem.* **1998**, 36, 955.
- [14] K. Matyjaszewski, S. G. Gaynor, A. Kulfan, M. Podwika, *Macromolecules* **1997**, 30, 5192.
- [15] K. Matyjaszewski, S. C. Gaynor, A. H. E. Müller, *Macromolecules* **1997**, 30, 7034.
- [16] K. Matyjaszewski, S. G. Gaynor, *Macromolecules* **1997**, 30, 7042.
- [17] H. Mori, D. C. Seng, H. Lechner, M. Zhang, A. H. E. Müller, *Macromolecules* **2002**, 35, 9270.
- [18] C. J. Hawker, J. M. J. Fréchet, R. B. Grubbs, J. Dao, *J. Am. Chem. Soc.* **1995**, 117, 10763.
- [19] A. Sunder, R. Hanselmann, H. Frey, R. Mülhaupt, *Macromolecules* **1999**, 32, 4240.
- [20] D. Baskaran, *Macromol. Chem. Phys.* **2001**, 202, 1569.
- [21] P. F. W. Simon, W. Radke, A. H. E. Müller, *Makromol. Chem., Rapid Commun.* **1997**, 18, 865.
- [22] K. Sakamoto, T. Aimiya, M. Kira, *Chem. Lett.* **1997**, 1245.
- [23] I. B. Dicker, G. M. Cohen, W. B. Farnham, W. R. Hertler, E. D. Laganis, D. Y. Sogah, *Macromolecules* **1990**, 23, 4034.
- [24] W. J. Middleton, *Org. Synth.* **1985**, 64, 221.
- [25] O. W. Webster, W. R. Hertler, D. Y. Sogah, W. B. Farnham, T. V. RajanBabu, *J. Am. Chem. Soc.* **1983**, 105, 5706.
- [26] W. R. Hertler, D. Y. Sogah, O. W. Webster, B. M. Trost, *Macromolecules* **1984**, 17, 1415.
- [27] W. J. Brittain, I. B. Dicker, *Macromolecules* **1989**, 22, 1054.
- [28] K. Dušek, J. Šomvářsky, M. Smrcková, W. J. Simonick, L. Wilczek, *Polym. Bull. (Heidelberg, Ger.)* **1999**, 42, 489.
- [29] H. Galina, J. B. Lechowicz, K. Kaczmarek, *Macromol. Theory Simul.* **2001**, 10, 174.
- [30] D. Hölder, H. Frey, *Acta Polym.* **1997**, 48, 298.
- [31] W. Radke, G. I. Litvinenko, A. H. E. Müller, *Macromolecules* **1998**, 31, 239.
- [32] D. Yan, Z. Zhou, *Macromolecules* **1999**, 32, 819.
- [33] A. D. Jenkins, E. Tsartolia, D. R. M. Walton, J. Horská-Jenkins, P. Kratochvil, J. Stejskal, *Makromol. Chem.* **1990**, 191, 2511.
- [34] D. Doskocilová, B. Schneider, J. Stoker, S. Sevcik, M. Prádný, L. Lochmann, *Makromol. Chem.* **1985**, 186, 1905.
- [35] D. Yan, A. H. E. Müller, K. Matyjaszewski, *Macromolecules* **1997**, 30, 7024.
- [36] A. H. E. Müller, R. Zhuang, D. Y. Yan, G. Litvinenko, *Macromolecules* **1995**, 28, 4326.
- [37] M. A. Doherty, A. H. E. Müller, *Makromol. Chem.* **1989**, 190, 527.